RESEARCH



Inferences on the Watts-Strogatz Model: A Study on Brain Functional Connectivity

Allan Falconi-Souto¹ · Rodrigo M. Cabral-Carvalho¹ · André Fujita^{2,3} · João Ricardo Sato⁴

Received: 3 June 2025 / Accepted: 4 November 2025 © The Author(s), under exclusive licence to Springer Science+Business Media, LLC, part of Springer Nature 2025

Abstract

Modelling real-world networks allows investigating the structure and the dynamics of such networks, which led to significant developments in various scientific fields. One of the most used models in these investigations is the Watts-Strogatz, with a structure composed of high clustering and short path lengths known as small-world networks. This model proposes an interesting gradient between regular and random networks, but its generating process, which relies on a single rewiring probability parameter, is hard to access and to manipulate. In order to study the mechanics of the Watts-Strogatz model, the present work proposes a new method based on deep neural networks that could estimate its probability p. To illustrate its applicability, neuroimaging and phenotypic resting-state fMRI data were used from patients with ADHD and typical development children, obtained from the ADHD-200 database. The neural network efficiently estimated the probability parameter, resulting in small-world graphs for functional brain connectivity with a mean \pm s.e.m. p distribution of 0.804 ± 0.003 . Despite no difference was found considering the gender or diagnosis of participants, the generalized linear model revealed age as a significant predictor of p (mean \pm s.e.m.: 4.410 ± 0.877 ; p<<0.001), indicating a great effect of neurodevelopment on the brain network's structure. The proposed approach is promising in estimating the probability of the Watts-Strogatz model, and its application has the potential to improve investigations of network connectivity with a relatively efficient and simple framework.

Keywords Watts-Strogatz model · Deep neural network · ADHD-200 · Functional connectivity

Lead ParagraphWe used machine learning principles to train a network to estimate a generative parameter for small-world network models. As such graphs can be used to model brain connectivity, we illustrate the trained neural network usefulness in a database of functional neuroimage, showing that this method can be easily applied to provide additional analysis and insights regarding the generative process of graph models.

Allan Falconi-Souto allan.falconi@ufabc.edu.br

Published online: 27 November 2025

- Postgraduate Program in Neuroscience and Cognition, Federal University of ABC, Alameda da Universidade, SN, São Bernardo do Campo, São Paulo, SP 09606-045, Brazil
- Department of Computer Science, Institute of Mathematics and Statistics, University of São Paulo, São Paulo, SP, Brazil
- Division of Network AI Statistics. Medical Institute of Bioregulation, Kyushu University, Fukuoka, Japan
- Center for Mathematics, Computing and Cognition, Federal University of ABC, São Bernardo do Campo, SP, Brazil

Introduction

Understanding real-world networks is essential in many fields (Jha et al., 2022; Patel et al., 2024; van den Heuvel & Hulshoff Pol, 2010; Verma et al., 2022). However, studying their structure can be difficult. For instance, even people with the same characteristics may have different brain activity patterns and functional brain networks. Another example is the metabolic networks that can differ between individuals in the same group. Because of this variability, networks can be seen as random graphs, reflecting underlying random processes.

Many models have been created to describe how networks form randomly. One of the first of random graphs models is the Erdős–Rényi (Erdös & Rényi, 1959), where each pair of nodes is connected with a fixed probability p. A more flexible version allows different probabilities p(i, j) for each pair of nodes (i, j). Researchers later introduced stochastic block models (SBM) to better comprehend realworld structures (Frank & Harary, 1982; Lee & Wilkinson,



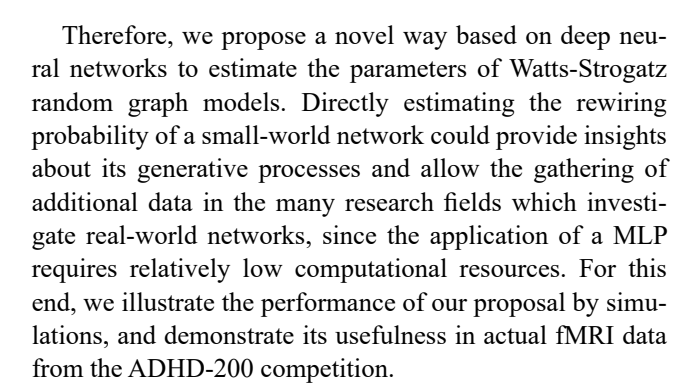
2019; Ludkin et al., 2018; Mariadassou & Tabouy, 2020). The deterministic block model assumes completely independent connections, while the SBM considers connections that depend on the group assignments of nodes.

Network models go beyond simple connections between nodes and capture other structural properties. For example, some models consider spatial relationships, like the geometric random graph (Duchemin & De Castro, 2023), while others enforce a fixed number of connections per node, such as the *d*-regular graph (Huang & Yau, 2023). The Watts–Strogatz (WS) model represents small-world networks (Watts & Strogatz, 1998), while the Barabási–Albert model captures networks with a power-law degree distribution (Barabási, 1999). The exponential random graph model (ERGM), a more flexible approach, defines connections based on chosen network statistics and external factors (Chatterjee & Diaconis, 2013).

Particularly, the Watts-Strogatz model (Watts & Strogatz, 1998) is a vital network science model that explains the small-world effect in many real-world networks. It shows how networks can have high clustering (like regular networks) and short path lengths (like random networks). This balance makes it helpful in studying networks such as brain connections, social relationships, neural systems, and the Internet. The model helps researchers understand, simulate, and analyze how these networks form and function.

However, there is no exact formula for estimating the parameters of the Watts-Strogatz model. Some models, like ER, SBM, and ERGM, have well-known parameter estimation methods. Although they are essential, these estimators only work for their specific models, so new estimation techniques must be developed every time a new network model is proposed. Thus, one of the main challenges in network analysis is creating a general way to determine the best model parameters for a given real-world network.

Takahashi et al. (2012) developed a general method to estimate the parameters of random graph models using the Kullback-Leibler divergence between graph spectral densities. This method also successfully estimated the parameter of the Watts-Strogatz model. Their proposal is based on the idea that a network's spectrum is closely related to its structure (Gera et al., 2018). Later, Siqueira Santos et al. (2021) proved the consistency of Takahashi et al.'s parameter estimator using the L1 norm instead of the Kullback-Leibler divergence. Nonetheless, this approach is not algorithmically efficient and exhibits poor scalability in high-dimensional settings. In contrast, matrix multiplication - fundamental to neural network architectures such as the Multilayer Perceptron – offers significantly greater computational efficiency and scalability, particularly due to its amenability to parallelization on GPUs.



Methodology

The Watts-Strogatz Model

The Watts-Strogatz model generates small-world networks exhibiting high clustering and short average path lengths. The Watts-Strogatz model starts with a regular ring lattice and rewires each edge with a given probability p, introducing randomness while maintaining some structure. Let N be the number of nodes, K/2 be the number of connected neighbors each node connects to on each side (K/2 must be even), and p be the probability of rewiring each edge. First, create a ring lattice, i.e., place N nodes in a circle and connect each node to its K/2 nearest neighbors on both sides. Then, for each edge (u, v), with probability p, rewire the edge, i.e., select a new target node v randomly (avoiding self-loops and duplicate edges) and replace the edge (u, v) with (u, v). After rewiring all the edges, a small-world network is obtained.

The Watts-Strogatz network model has some interesting properties related to the small-world effect seen in many real-world networks. For example, when p=0, we obtain a regular ring lattice, i.e., a network with high clustering and long path lengths. When 0 , we get a small-world network, i.e., a network with high clustering and short path lengths. Finally, when <math>p=1, we obtain a random graph, i.e., low clustering and short path lengths.

Deep Neural Networks and P Estimation

A neural network is trained on datasets generated from simulations of the Watts-Strogatz model, specifically, a Multi-Layer Perceptron (MLP), a neural network model to tackle a specific predictive task. An MLP is a fundamental form of neural network composed of typically three layers of neurons connected through weighted pathways: (1) an input layer that receives the data – in this case a connective matrix; (2) the hidden layers, which computes and transforms the data; and (3) an output layer that returns the



Neuroinformatics (2025) 23:57 Page 3 of 8 57

desired prediction (Naskath et al., 2023). The current model architecturally consists of three densely connected hidden layers – composed of 50, 20 and 10 neurons, respectively – with a Rectified Linear Unit (ReLU; Eq. 1) activation function, culminating in a single neuron output layer that uses a Scaled Exponential Linear Unit (SeLU; Eq. 2) activation function to produce the final estimation. The general architecture of the MLP is represented in Fig. 1.

$$ReLU(x) = \begin{cases} x, & \text{if } x > 0 \\ 0, & \text{if } x \le 0 \end{cases}$$
 (1)

$$SeLU(x) = \lambda \begin{cases} x, & \text{if } x > 0 \\ \alpha e^x - \alpha, & \text{if } x \le 0 \end{cases}$$
 (2)

The primary focus of the training is to estimate the parameter p, which represents the probability of rewiring each edge within the model, dictating the randomness or regularity of the network structure. This type of idea of training on simulations to evaluate numerical quantities of empirical data (Tobin et al., 2017; Cranmer et al., 2020) has already been applied to resting-state fMRI functional connectivity (Cabral-Carvalho et al., 2025). However, the use of a MLP has not yet been investigated as a possible methodology for estimating these numerical quantities. The training dataset comprises 10,000 Watts Strogatz model simulations with 100 nodes, and the test set has 1,000 samples. The training employs the Adam optimizer for its efficiency in managing sparse gradients and uses Mean Absolute Error (MAE) as the loss function. The model was trained over 100 epochs

Fig. 1 Representation of the designed MLP

with a learning rate of l=0.001, and it was built with the Tensorflow and Keras framework.

Illustrative Simulations

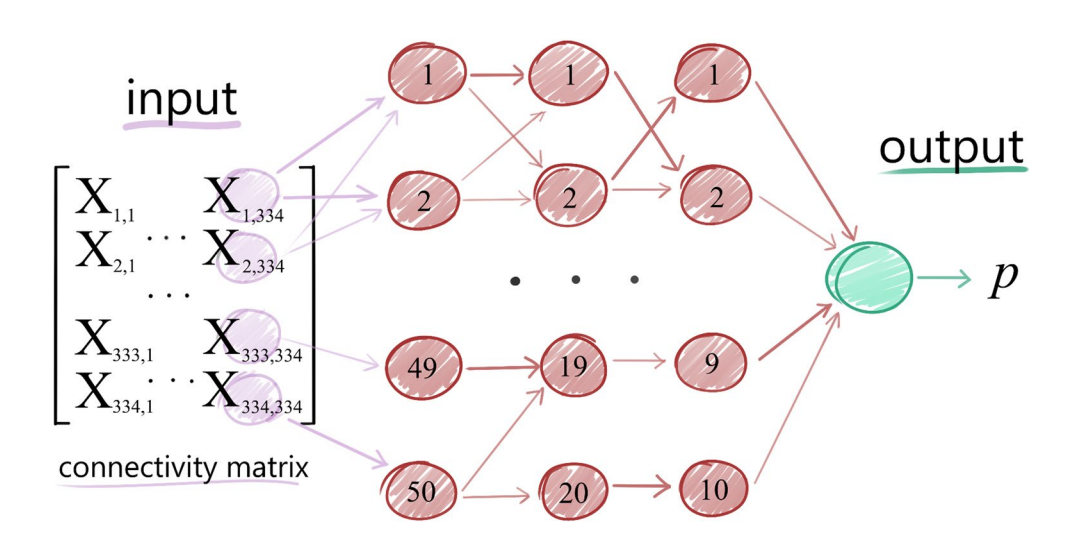
Monte Carlo simulations were used to illustrate the proposed approach's performance. Since the typical brain parcellation in fMRI studies involves hundreds of cortical regions, we simulated graphs with 50, 100 and 200 nodes. The average number of neighbours was set to 5%, 10%, and 20% of the respective number of nodes. The Pearson correlation coefficient *r* is calculated as a precision metric.

ADHD-200 Dataset

In this study, we analyzed resting-state functional magnetic resonance imaging (fMRI) data sourced from the publicly available ADHD-200 dataset provided by the Neuro Bureau. This dataset, described comprehensively in Bellec et al. (2017), consolidates data collected across eight centers using 1.5 Tesla MRI scanners. Participants were initially classified into four diagnostic categories: healthy controls, ADHD combined subtype, ADHD hyperactive-impulsive subtype, and ADHD inattentive subtype. In addition to neuroimaging data, detailed phenotypic information was provided, including age, gender, handedness, IQ, and specific ADHD subtype classification.

The data preprocessing was performed using the Athena pipeline, explicitly designed for resting-state fMRI and voxel-based morphometry (grey matter) analysis, implemented via AFNI and FSL software tools (Bellec et al., 2017). The preprocessed data were retrieved from the Connectome website (www.preprocessed-connectomes-proje ct.org/adhd200/) and included resting-state BOLD signal

hidden layer





time courses. The preprocessing steps consisted of discarding the first four volumes to achieve magnetic stabilization, slice timing correction, head motion correction, spatial normalization to Montreal Neurological Institute (MNI) standard space at $4\times4\times4$ mm voxel resolution, temporal band-pass filtering (0.009–0.08 Hz), and spatial smoothing with a Gaussian kernel of 6 mm full width at half maximum (FWHM). Further methodological details, including site-specific MRI scanner parameters, are thoroughly documented on the ADHD-200 website (ADHD-200-Webpage, 2011). We included only the initial scan for participants with multiple scanning sessions and uniformly extracted 140 time points for each subject.

Excluding phenotypic missing data, the sample utilized for the illustrative application had a total of 525 individuals. Sex differences in age distribution were examined, and their mean \pm standard deviation are described as follows, revealing similar ages for males (12.19 \pm 3.47 years) and females (12.293 \pm 3.818 years). The impact of the ADHD subtype on age distribution was also assessed, yielding mean ages as follows: Typically Developing Children, 12.567 \pm 3.69 years years; ADHD-Combined subtype, 11.358 \pm 3.4 years years; ADHD-Hyperactive/Impulsive subtype, 13.371 \pm 4.533 years; and ADHD-Inattentive subtype, 11.628 \pm 2.943 years.

Illustrative Application

For the functional connectivity analysis, matrices were created from the ADHD-200 dataset. Those connectivity matrices consisted of a 334×334 matrix for each subject, with connectivity indexes considered as present (1) if equal or greater than 0.2, or absent (0), otherwise. The connectivity matrices were submitted to the neural network, which then simulated different matrices with the same N and k to estimate the probability p for the entry matrix correctly. Considering these estimated p as dependent variable, a generalized linear model (GLM) was applied, with site of data collection, and subject's gender, age, diagnosis (ADHD(C): ADHD-Combined subtype; ADHD(H/I): ADHD-Hyperactive/Impulsive subtype; ADHD-I: ADHD-Inattentive subtype) and frame displacement (FD) as predictors (Eq. 3). A significance level of 0.05 was adopted.

$$Y_{i} = \beta_{0} + \beta_{1} \cdot \operatorname{gender}_{i} + \beta_{2} \cdot \operatorname{age}_{i} + \beta_{3} \cdot \operatorname{ADHD}(C)_{i} + \beta_{4} \cdot \operatorname{ADHD}(H/I)_{i} + \beta_{5} \cdot \operatorname{ADHD}(I)_{i} + \beta_{6} \cdot \operatorname{FD}_{i} + \epsilon_{i}$$
(3)



Simulations

The simulation results are shown in Fig. 2. First, note that the proposed strategy for p estimation is effective and provides accurate results in graphs with a scale of 50, 100 and 200 nodes. Moreover, since more information is available, when the number of nodes N or the number of neighbours k increases, the quality of the estimate improves, mainly because variability is reduced.

Application in ADHD-200 Dataset

The artificial neural network designed in this study could estimate a probability p for all tested connectivity matrices of the ADHD-200 dataset. The general estimated p was 0.804 ± 0.003 (mean \pm s.e.m.; Fig. 3). Grouping the probability p for each participant according to their gender (Fig. 4) or diagnosis (Fig. 5) shows almost no difference in p distribution among these groups.

Indeed, the generalized linear model found no significant difference for gender or diagnosis (Table 1). However, a significant effect of both subjects' age and frame displacement on the p distribution was found, meaning that these variables may be considered predictors of p.

Discussion

In the present study, functional neuroimaging data from ADHD patients were used to illustrate the applicability of a deep neural network in estimating a graph's rewiring probability p, a main parameter of the small-world model proposed by Watts and Strogatz (1998). We found no significant result regarding the connectivity matrices' p when grouped by patients' diagnosis or gender. On the other hand, parameter p was positively correlated to the individual's age. Consequently, the connection between functional brain areas would tend to be less clustered and with shorter path length as an individual transitions from infancy to adulthood. Such comprehension of the network's generating process, and how its rewiring probability affects the network features, could only be carried out with the estimation of p, which is the method proposed in this study.

Intense developmental changes in the nervous system mark childhood and adolescence. Especially during puberty, synaptic strengthening and pruning processes change the brain organization and affect cognitive and socioemotional processes (see Vijayakumar et al., 2018). In this line, by modeling the brain as a small-world network, Zhao et al. (2015) found that both the path length and clustering



Neuroinformatics (2025) 23:57 Page 5 of 8 57

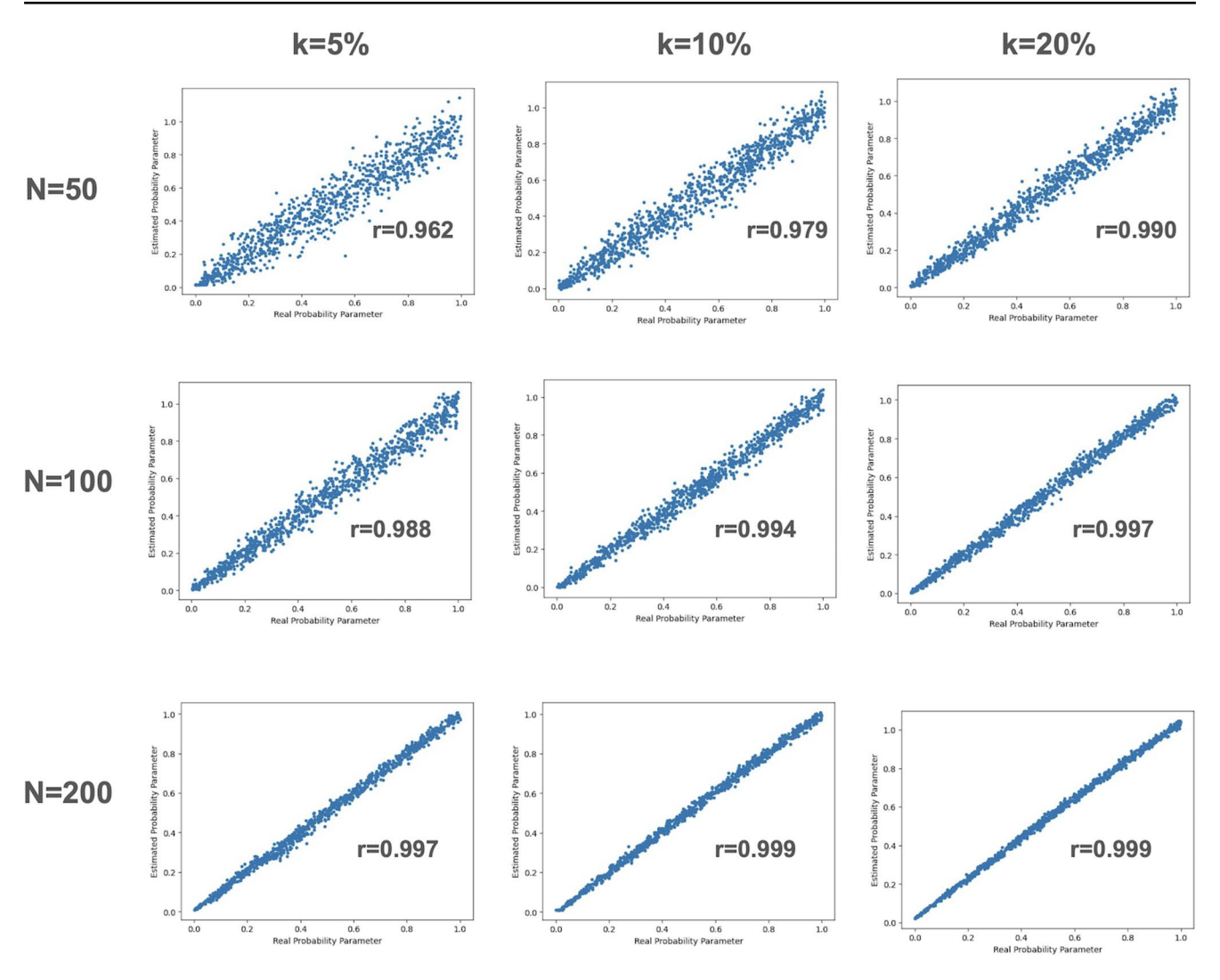


Fig. 2 Simulations results. Scatter-plot between estimated and actual p parameter for different values of the number of nodes (N) and the mean number of neighbours (k, a) as a percentage of the number of nodes).

Note that the variability of estimates is reduced when both N and k increase. The coefficient \mathbf{r} is the Pearson correlation value between estimated and actual \mathbf{p} parameters

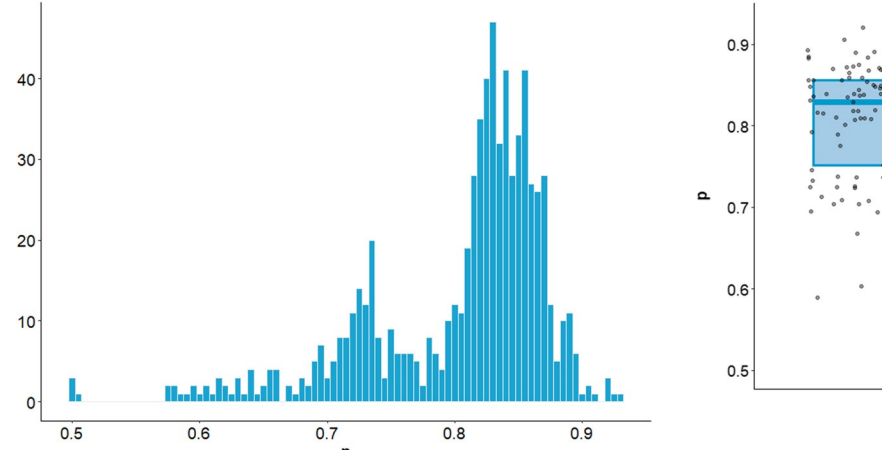


Fig. 3 Distribution of probability p

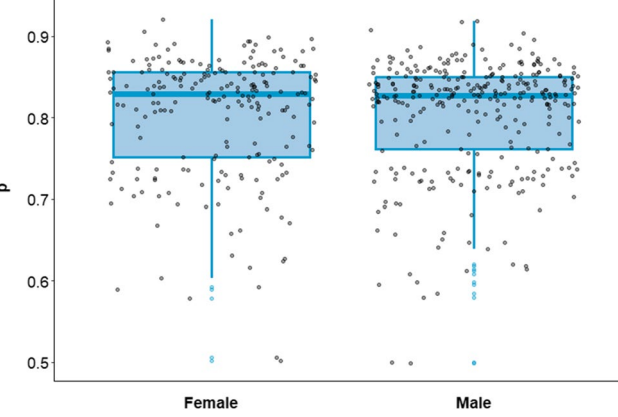


Fig. 4 Distribution of p for each gender



57 Page 6 of 8 Neuroinformatics (2025) 23:57

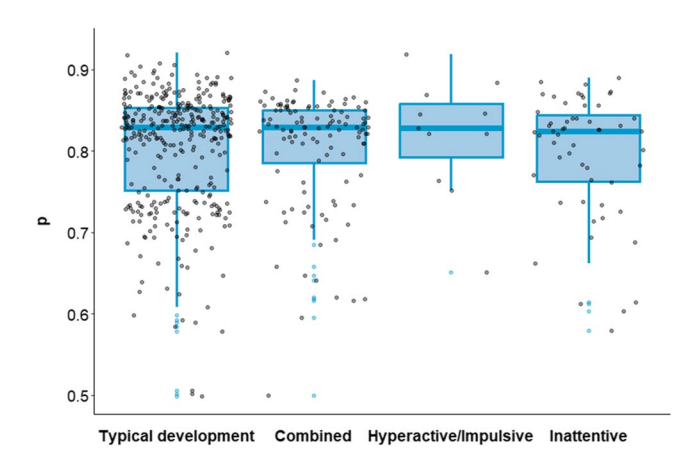


Fig. 5 Distribution of p for each ADHD diagnosis

Table 1 General linear model considering p as dependent variable

Table 1 Semeral mean relationship as dependent variable		
Parameter	Estimate (e-3)	<i>p</i> -value
Gender (male)	-1.261 ± 6.564	0.847
Age	4.410 ± 0.877	<0.001 ***
Diagnosis (ADHD-Combined)	$6.022\!\pm\!8.073$	0.456
Diagnosis (ADHD-Hyperactive/ Impulsive)	13.54 ± 21.89	0.536
Diagnosis (ADHD-Inattentive)	-4.169 ± 10.42	0.689
Frame displacement	-0.003 ± 0.001	0.009 **

Values are expressed as mean ± standard error.

coefficient of the white matter network follow an inverted U pattern, with a peak at the third decade related to the maturation of these structures. There is, however, a gap in understanding the relationship between structural and functional connectivity, as functional networks present a more complex behavior, quickly changing its organization over time and being able to act upon indirect structural connections, for example (Liao et al., 2017).

In this context, Gu et al. (2015) showed that cognitive systems tend to differentiate along development and establish their functional roles. Their results indicate a decrease in global between-system connectivity, but some modules do the opposite, especially the default mode network and the sensorimotor system. In this sense, the increase of a between-system connectivity suggests a diversification of functions performed by each brain region and would imply a shortening in the network's path length. On the other hand, Smit et al.'s (2012) results of EEG activity indicate a network's pattern towards order, as the alpha, beta and theta frequency bands had an increase in both clustering and path length over age: they only showed a shift to randomness in an older age (55+).

It is important to note that all these studies investigated only the path length and the clustering coefficient, which are described as functions of the network models' rewiring probability p. By directly accessing p from the functional connectivity graphs, the methods presented in this study indicate that these networks' features variates with age, which, in turn, can be explained by variations in the model's rewiring probability p.

Despite there being no difference found regarding the estimated p and the ADHD diagnosis, several studies indicate that such disorder profoundly affects the brain connectivity. Beare et al. (2017), through a graph theory-based approach, found that the white matter network of children and adolescents diagnosed with ADHD had a higher clustering coefficient and weighted normalized path length compared to typically developing controls. Differences between groups' networks features were also found regarding functional connectivity: Wang et al. (2019), however, found that both normalized clustering coefficient and path length were reduced in diagnosed children from the ADHD-200 database. Furthermore, such changes seem to be dependent on the subtype of ADHD, as the structure of brain networks for Inattentive and Combined subtypes does not differ from control or even between these diagnoses (Saad et al., 2021).

Even so, the estimated value and its possible impact on brain functioning analysis need further investigation, as their values are limited by the parameters used in the deep neural network implementation. For example, a fixed threshold affects the graph's parameters, changing its structure according to the connectivity values (Telesford et al., 2011). Hence, one of the limitations of the present study is to adequately address the weights of the connections or even the usage of a gradient of possible thresholds. Future studies may complement their data collection and network modelling with the methods proposed in this paper, and help to address the proper applicability of such an approach in studying brain connectivity.

Conclusion

The deep neural network proposed in this study could directly estimate the probability p of a Watts-Strogatz model. Using a brain functional connectivity database, the network application could provide new information on the graph's structure, pointing to the relevance of neurodevelopmental processes in the brain's functionality. Such an analysis could be easily implemented in future research, expanding the knowledge of its applicability and the investigated graph's structure. However, some parameters of the neural network function, such as defining an optimal threshold for connectivity data, still need to be considered when implementing such a methodology.

Acknowledgements This study is supported by the São Paulo Research Foundation (FAPESP) Grants 2021/05332-8, 2023/02616-0,



Neuroinformatics (2025) 23:57 Page 7 of 8 57

2023/02538-0, and 2024/03261-4, and the MEXT Cooperative Research Project Program, Medical Research Center Initiative for High-Depth Omics and CURE: JPMXP1323015486 for MIB, Kyushu University.

Author Contributions All authors read and agreed to the manuscript's final format. Specific contributions are described as follows: AF-S: Investigation; visualization; writing; RMC: Writing; AF: Writing; JRS: Conceptualization; methodology; supervision; writing.

Data Availability The data that support the findings of this study are available from the Neuro Bureau. Restrictions apply to the availability of these data, which were used under license for this study. Data are available from the authors upon reasonable request and with the permission of the Neuro Bureau.

Declarations

Competing interests The authors declare no competing interests.

References

- Barabási, A. (1999). Emergence of scaling in random networks. *Science*, 286(5439), 509–512. https://doi.org/10.1126/science.286.5439.509
- Beare, R., Adamson, C., Bellgrove, M. A., Vilgis, V., Vance, A., Seal, M. L., & Silk, T. J. (2017). Altered structural connectivity in ADHD: A network based analysis. *Brain Imaging and Behavior*, 11(3), 846–858. https://doi.org/10.1007/s11682-016-9559-9
- Bellec, P., Chu, C., Chouinard-Decorte, F., Benhajali, Y., Margulies, D. S., & Craddock, R. C. (2017). The neuro bureau ADHD-200 preprocessed repository. *Neuroimage*, 144(Part B), 275–286. https://doi.org/10.1016/j.neuroimage.2016.06.034
- Cabral-Carvalho, R., Pinaya, W., & Sato, J. (2025). A graph neural network approach to investigate brain critical States over neurodevelopment. *Network Neuroscience*. https://doi.org/10.1162/net n_a_00451
- Chatterjee, S., & Diaconis, P. (2013). Estimating and Understanding exponential random graph models. *The Annals of Statistics*, 41(5), 2428–2461. https://doi.org/10.1214/13-AOS1155
- Cranmer, K., Brehmer, J., & Louppe, G. (2020). The frontier of simulation-based inference. Proceedings of the National Academy of Sciences, 117(48), 30055–30062. https://doi.org/10.1073/pnas.1912789117
- Duchemin, Q., & De Castro, Y. (2023). Random geometric graph: Some recent developments and perspectives. In R. Adamczak, N. Gozlan, K. Lounici, & M. Madiman (Eds.), *High dimensional* probability IX. Progress in probability, vol 80 (pp. 347–392). Birkhäuser. https://doi.org/10.1007/978-3-031-26979-0_14
- Erdös, P., & Rényi, A. (1959). On random graphs I. *Publicationes Mathematicae Debrecen*, 6, 290–297.
- Frank, O., & Harary, F. (1982). Cluster inference by using transitivity indices in empirical graphs. *Journal of the American Statistical Association*, 77(380), 835–840. https://doi.org/10.1080/0162145 9.1982.10477895
- Gera, R., Alonso, L., Crawford, B., House, J., Mendez-Bermudez, J. A., Knuth, T., & Miller, R. (2018). Identifying network structure similarity using spectral graph theory. *Applied Network Science*, 3, 2. https://doi.org/10.1007/s41109-017-0042-3
- Gu, S., Satterthwaite, T. D., Medaglia, J. D., Yang, M., Gur, R. E., Gur, R. C., & Bassett, D. S. (2015). Emergence of system roles in normative neurodevelopment. *Proceedings of the National*

- Academy of Sciences of the United States of America, 112(44), 13681–13686. https://doi.org/10.1073/pnas.1502829112
- Huang, J., & Yau, H. (2023). Spectrum of random d-regular graphs up to the edge. *Communications on Pure and Applied Mathematics*, 77(3), 1635–1723. https://doi.org/10.1002/cpa.22176
- Jha, K., Saha, S., & Singh, H. (2022). Prediction of protein–protein interaction using graph neural networks. *Scientific Reports*, 12, 8360. https://doi.org/10.1038/s41598-022-12201-9
- Lee, C., & Wilkinson, D. J. (2019). A review of stochastic block models and extensions for graph clustering. *Applied Network Science*, 4, 122. https://doi.org/10.1007/s41109-019-0232-2
- Liao, X., Vasilakos, A. V., & He, Y. (2017). Small-world human brain networks: Perspectives and challenges. *Neuroscience and Biobe-havioral Reviews*, 77, 286–300. https://doi.org/10.1016/j.neubiorev.2017.03.018
- Ludkin, M., Eckley, I., & Neal, P. (2018). Dynamic stochastic block models: Parameter Estimation and detection of changes in community structure. *Statistics and Computing*, 28, 1201–1213. https://doi.org/10.1007/s11222-017-9788-9
- Mariadassou, M., & Tabouy, T. (2020). Consistency and asymptotic normality of stochastic block models estimators from sampled data. *Electronic Journal of Statistics*, *14*(2), 3672–3704. https://doi.org/10.1214/20-EJS1750
- Naskath, J., Sivakamasundari, G., & Begum, A. A. S. (2023). A study on different deep learning algorithms used in deep neural nets: MLP SOM and DBN. Wireless Personal Communications, 128(4), 2913–2936. https://doi.org/10.1007/s11277-022-10079-4
- Patel, A. C., Sinha, S., & Palermo, G. (2024). Graph theory approaches for molecular dynamics simulations. *Quarterly Reviews of Biophysics*, 57, e15. https://doi.org/10.1017/S0033583524000143
- Saad, J. F., Griffiths, K. R., Kohn, M. R., Braund, T. A., Clarke, S., Williams, L. M., & Korgaonkar, M. S. (2021). No support for white matter connectivity differences in the combined and inattentive ADHD presentations. *Plos One*, 16(5), e0245028. https:// doi.org/10.1371/journal.pone.0245028
- Siqueira Santos, S., Fujita, A., & Matias, C. (2021). Spectral density of random graphs: Convergence properties and application in model fitting. *Journal of Complex Networks*, 9(6), cnab041. https://doi.org/10.1093/comnet/cnab041
- Smit, D. J., Boersma, M., Schnack, H. G., Micheloyannis, S., Boomsma, D. I., Pol, H., Stam, H. E., C. J., & de Geus, E. J. (2012). The brain matures with stronger functional connectivity and decreased randomness of its network. *Plos One*, 7(5), e36896. https://doi.org/10.1371/journal.pone.0036896
- Takahashi, D. Y., Sato, J. R., Ferreira, C. E., & Fujita, A. (2012). Discriminating different classes of biological networks by analyzing the graphs spectra distribution. *Plos One*, 7(12), e49949. https://doi.org/10.1371/journal.pone.0049949
- Telesford, Q. K., Simpson, S. L., Burdette, J. H., Hayasaka, S., & Laurienti, P. J. (2011). The brain as a complex system: Using network science as a tool for Understanding the brain. *Brain Connectivity*, 1(4), 295–308. https://doi.org/10.1089/brain.2011.0055
- Tobin, J., Fong, R., Ray, A., Schneider, J., Zaremba, W., & Abbeel, P. (2017). Domain randomization for transferring deep neural networks from simulation to the real world. ArXiv. https://doi.org/10 .48550/ArXiv.1703.06907
- van den Heuvel, M. P., & Hulshoff Pol, H. E. (2010). Exploring the brain network: A review on resting-state fMRI functional connectivity. European Neuropsychopharmacology: the Journal of the European College of Neuropsychopharmacology, 20(8), 519– 534. https://doi.org/10.1016/j.euroneuro.2010.03.008
- Verma, R. K., Shinde, P., & Jalan, S. (2022). Nucleotide-based genetic networks: Methods and applications. *Journal of Biosciences*, 47(4), 63. https://doi.org/10.1007/s12038-022-00290-7
- Vijayakumar, N., de Macks, O., Shirtcliff, Z., E. A., & Pfeifer, J. H. (2018). Puberty and the human brain: Insights into adolescent



development. Neuroscience and Biobehavioral Reviews, 92, 417–436. https://doi.org/10.1016/j.neubiorev.2018.06.004

Wang, Y., Zuo, C., Xu, Q., Liao, S., Kanji, M., & Wang, D. (2019).
Altered resting functional network topology assessed using graph theory in youth with attention-deficit/hyperactivity disorder.
Progress in Neuropsychopharmacology & Biological Psychiatry, 98, 109796. https://doi.org/10.1016/j.pnpbp.2019.109796

Watts, D. J., & Strogatz, S. H. (1998). Collective dynamics of small-world networks. *Nature*, 393(6684), 440–442. https://doi.org/10.1038/30918

Zhao, T., Cao, M., Niu, H., Zuo, X. N., Evans, A., He, Y., Dong, Q., & Shu, N. (2015). Age-related changes in the topological organization of the white matter structural connectome across the human

lifespan. *Human Brain Mapping*, 36(10), 3777–3792. https://doi.org/10.1002/hbm.22877

Publisher's Note Springer Nature remains neutral with regard to jurisdictional claims in published maps and institutional affiliations.

Springer Nature or its licensor (e.g. a society or other partner) holds exclusive rights to this article under a publishing agreement with the author(s) or other rightsholder(s); author self-archiving of the accepted manuscript version of this article is solely governed by the terms of such publishing agreement and applicable law.

